Supplementary Figure 1

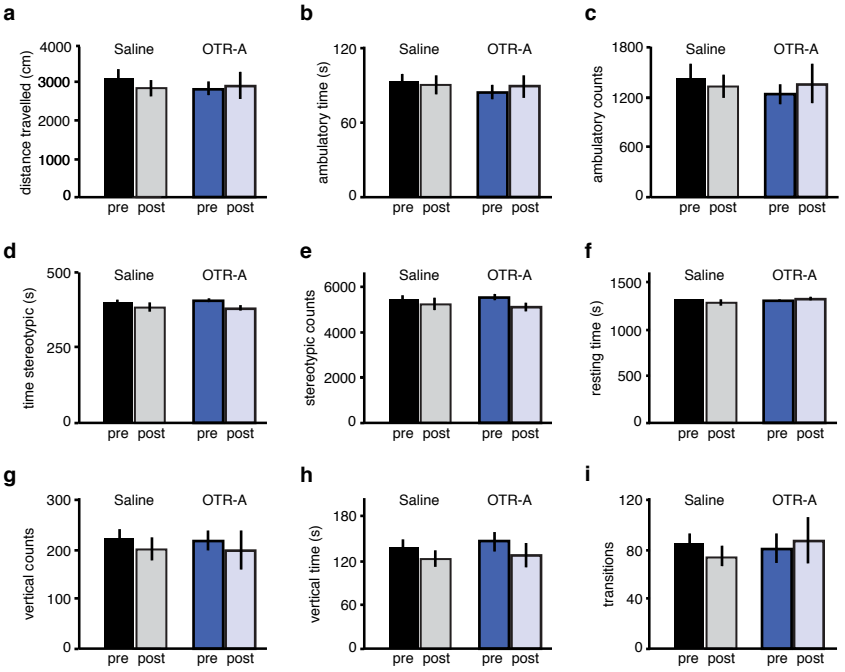

Supplementary Figure 1. Locomotor activity is not altered by sCPP or OTR-A. a-i, distance travelled (a), ambulatory time (b) ambulatory counts (c) time stereotypic (d) stereotypic counts (e) resting time (f) vertical counts (g) vertical time (h) and number of transitions (i) are not different between groups (saline injected, n = 15 - 18, OTR-A injected, n = 11 - 15).

Supplementary Figure 2

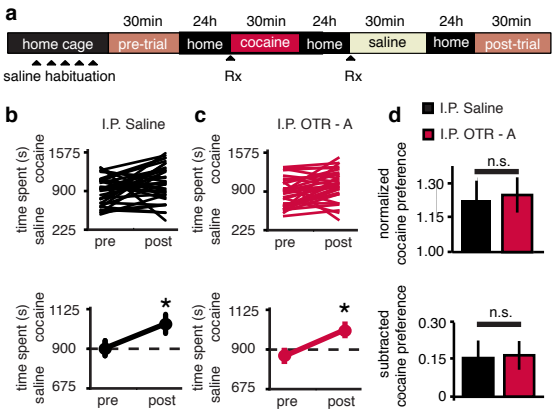

Supplementary Figure 2. Cocaine conditioned place preference (cCPP) does not require OT. a, Diagram illustrating time course of i.p. injections during cCPP experiments in **b-d**. **b,c** Individual (top) and average (bottom) preference scores (total time spent on cocaine cue/half the total time) indicate that animals receiving i.p. saline (**b**) or i.p. OTR-A (**c**) both have a significantly increased preference for the cocaine context after conditioning (i.p. saline injected, n = 34, i.p. OTR-A injected, n = 32). **d**, Comparisons between i.p. saline versus i.p. OTR-A treated animals reveals no difference in normalized cocaine preference and subtracted cocaine preference in OTR-A treated animals.

Supplementary Figure 3

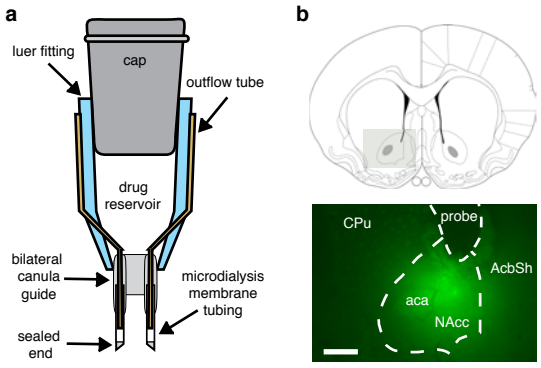

Supplementary Figure 3. Andalman reverse microdialysis probes. a, Schematic of Andalman probe for reverse microdialysis experiments in Fig. 1f-i and 5l-o. **b,** Post-hoc confirmation of probe placement and competency.

Supplementary Figure 4

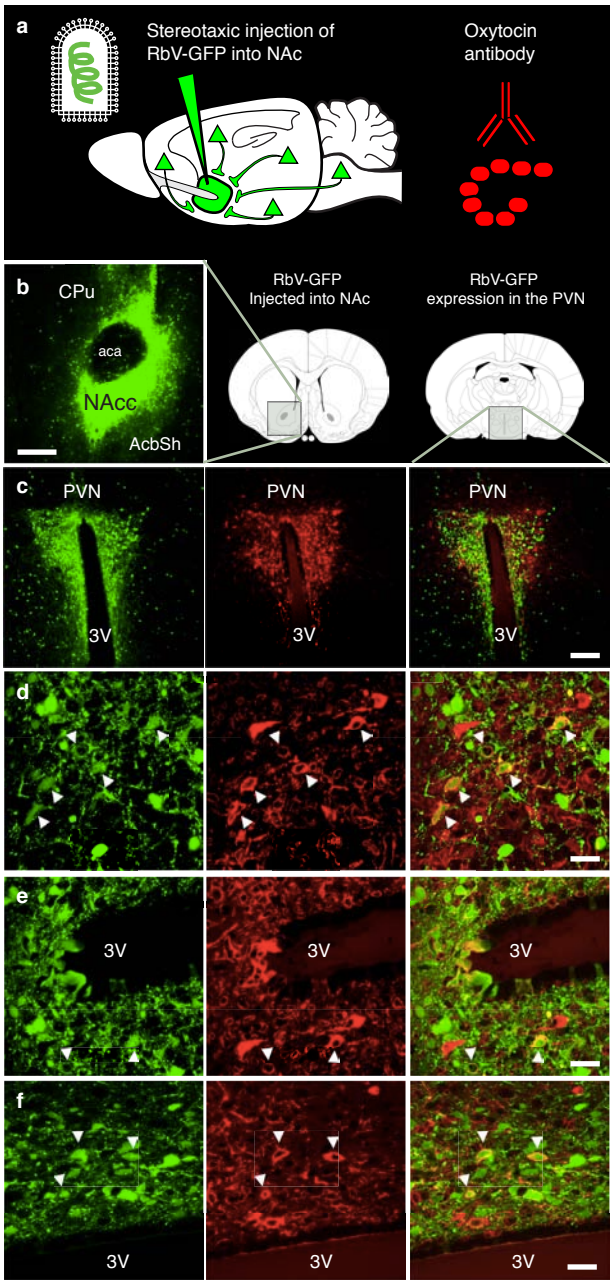

Supplementary Figure 4. OT expressing neurons in the paraventricular nucleus (PVN) send projections to the NAc. a, Diagram illustrating the injection of RbV-GFP into the NAc, followed by antibody labeling of OT producing neurons in the PVN. **b,** Localization and expression of RbV-GFP in the NAc (scale bars 200 μm). **c-f,** Low magnification (**c**,scale bar 100 μm) and high magnification **(d-f,** scale bars 20 μm) images of PVN cells that have been retrogradely labeled by RbV-GFP taken up by presynaptic terminals in the NAc (green, left panels) and labeled by ant-OT-np antibody (red, center panels). Co-localization (merged right panels) indicates oxytocinergic neurons that project to the NAc; arrowheads highlight individual cells that show co-localization. (Nucleus accumbens core, NAcc; nucleus accumbens shell, AcbSh; anterior commissure, aca; caudate putamen, CPu; third ventricle, 3V; paraventricular nucleus of the hypothalamus, PVN)

Supplementary Figure 5

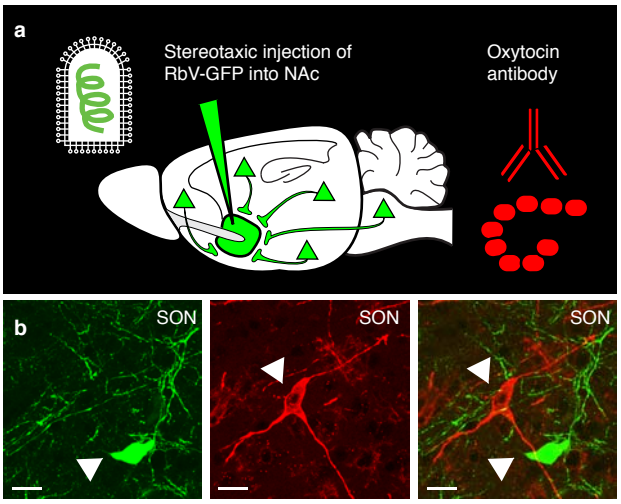

Supplementary Figure 5. OT expressing neurons in the Supraoptic Nucleus (SON) do not send projections to the NAc. a, Diagram illustrating the injection of RbV-GFP into the NAc, followed by antibody labeling of OT producing neurons in the PVN. **b,** high magnification (scale bars 20 μm) images of SON cells that have been retrogradely labeled by RbV-GFP taken up by presynaptic terminals in the NAc (green, left panels) or labeled by ant-OT-np antibody (red, center panels). Absence of co-localization (merged right panels) indicates oxytocinergic neurons do not project to the NAc.

Supplementary Figure 6

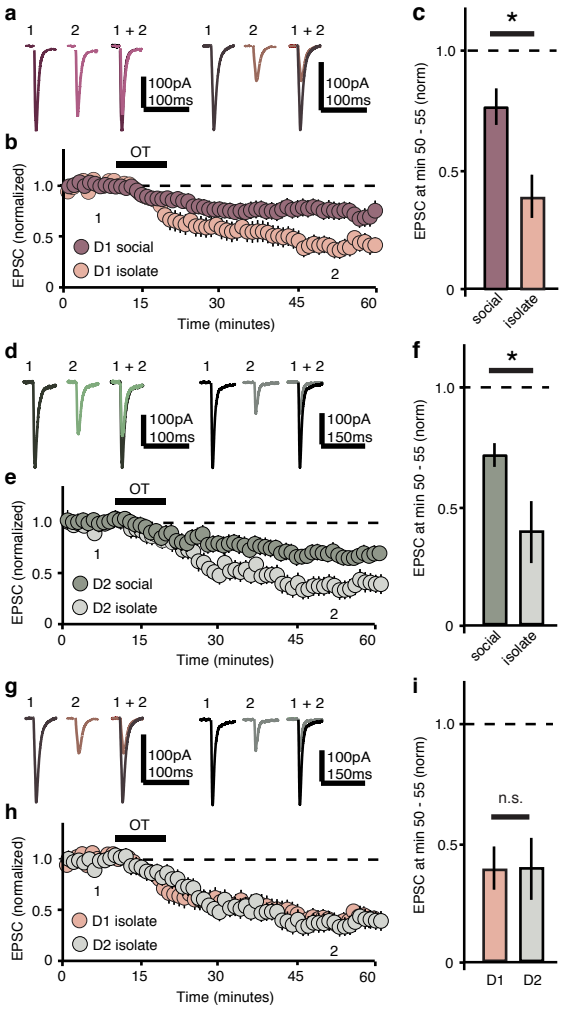

Supplementary Figure 6. Increased magnitude of OT-LTD in both D1 and D2 receptor expressing MSN following isolation conditioning. a-h, Representative traces **(a,d,g)**, summary time course **(b,e,h),** and average post-treatment magnitude comparisons **(c,f.i)** reveal that the magnitude of OT-LTD is significantly increased in both D1 **(a-c)** and D2 **(d-f)** cells from isolation versus socially reared animals (D1 isolation, n = 6 and D1 social n = 9 cells; D2 isolation, n = 5 and D2 social n = 11 cells); and the magnitude of EPSC OT-LTD is not different in D1 versus D2 MSNs from slices made from isolation conditioned animals (**g-i,** n = 6 D1, and n = 5 D2 cells).

Supplementary Figure 7

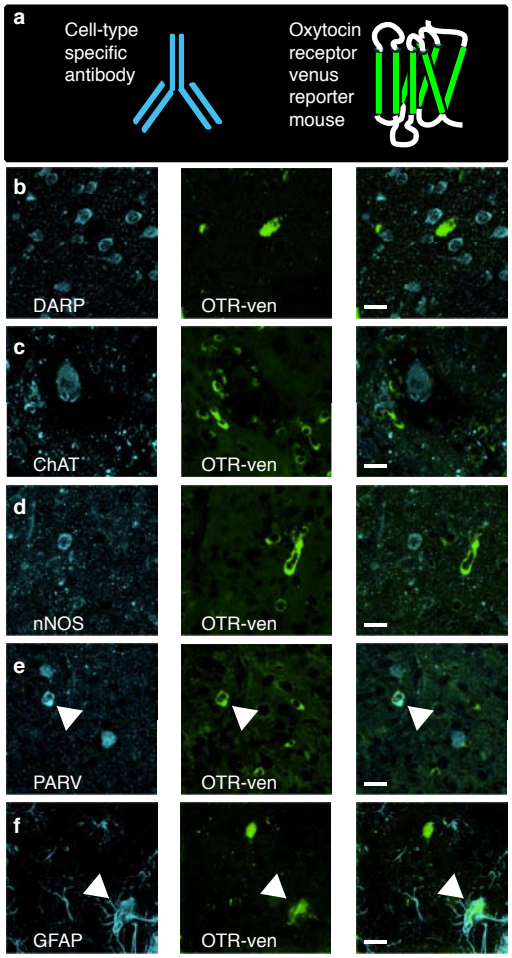

Supplementary Figure 7. OT receptor (OTR) expressing cells in the NAc. **a,** Diagram illustrating immunolabeling with cell-type specific antibodies in the NAc of OTR-Venus mice. **b,** DARP positive MSNs (blue, left) and OTR-Ven positive cells (green, center) do not co-localize (merge, right). **c,** CHAT positive cholinergic interneurons (blue, left) and OTR-Ven positive cells (green, center) do not co-localize (merge, right). **d,** nNOS positive inhibitory interneurons (blue, left) and OTR-Ven positive cells (green, center) do not co-localize (merge, right). **e,** a subset of PARV positive inhibitory interneurons (blue, left) and OTR-Venus positive cells (green, center) show co-localization (merge, right). **f,** a subset of GFAP positive glial cells (blue, left) and OTR-Ven positive cells (green, center) show co-localization (merge, right). (Scale bars 20 μm)

Supplementary Figure 8

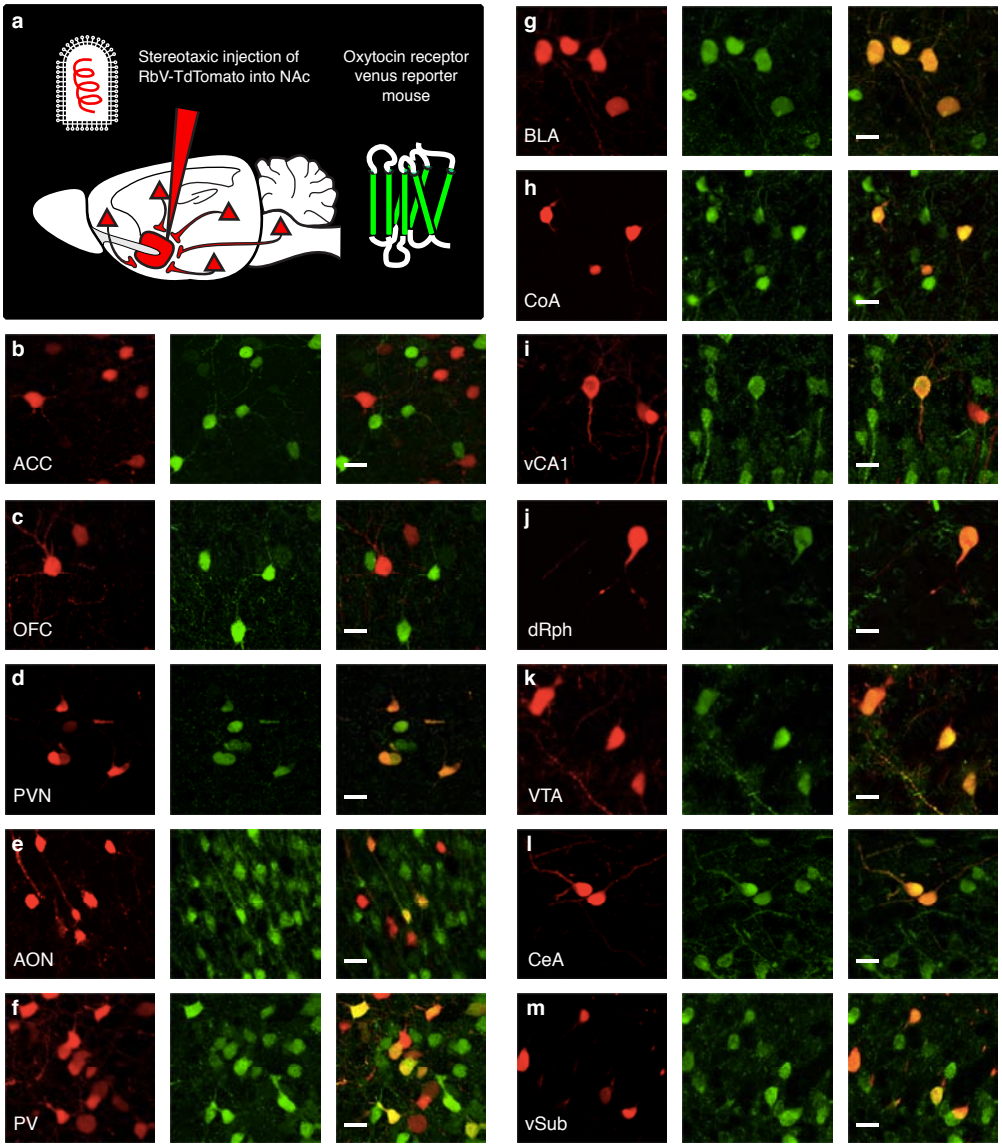

Supplementary Figure 8. OT receptor expressing cells that project to the NAc. a, Diagram illustrating stereotaxic injection of RbV-TdTomato into the NAc of OTR-Venus mice. **b-m,** high magnification images of cells in the (b) anterior cingulate cortex, ACC; (c) orbitofrontal cortex, OFC; (d) paraventricular nucleus of the hypothalamus, PVN; (e) anterior olfactory nucleus, AON; (f) paraventricular thalamus, PV; (g) basolateral amygdala, BLA; (h) cortex of the amygdala, CoA; (i) ventral hippocampal CA1, vCA1; (j) dorsal Raphe nucleus, dRph; (k) caudal ventral tegmental nucleus, VTA; (l) central amygdala, CeA; and ventral subiculum, vSub that have been retrogradely labeled by RbV-GFP taken up by presynaptic terminals in the NAc (red, left panels) and that express OTR-Venus (green, center panels). Co-localization (merge, right panels) is notably absent in (b) ACC and (c) OFC, but in all other regions (d-m), a subset of cells show clear co-localization (project to the NAc and express OTR-Venus), implicating these neurons as a putative source of presynaptic OTRs in the NAc. (Scale bars 20 µm).

Supplementary Figure 9

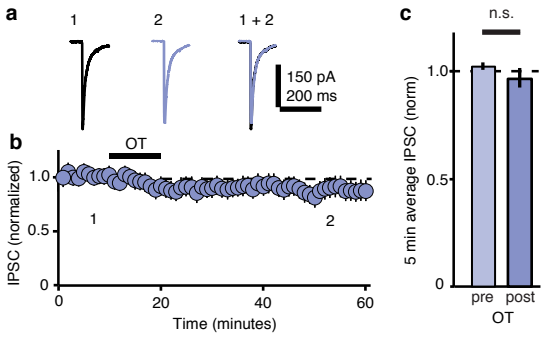

Supplementary Figure 9. OT does not alter inhibitory postsynaptic currents (IPSCs) recorded from NAc MSNs. Representative traces **(a)**, summary time course **(b)** and average post-treatment magnitude comparisons **(c)** reveal absence of significant OT-induced changes in IPSC amplitude (n = 11 cells).

Supplementary Figure 10

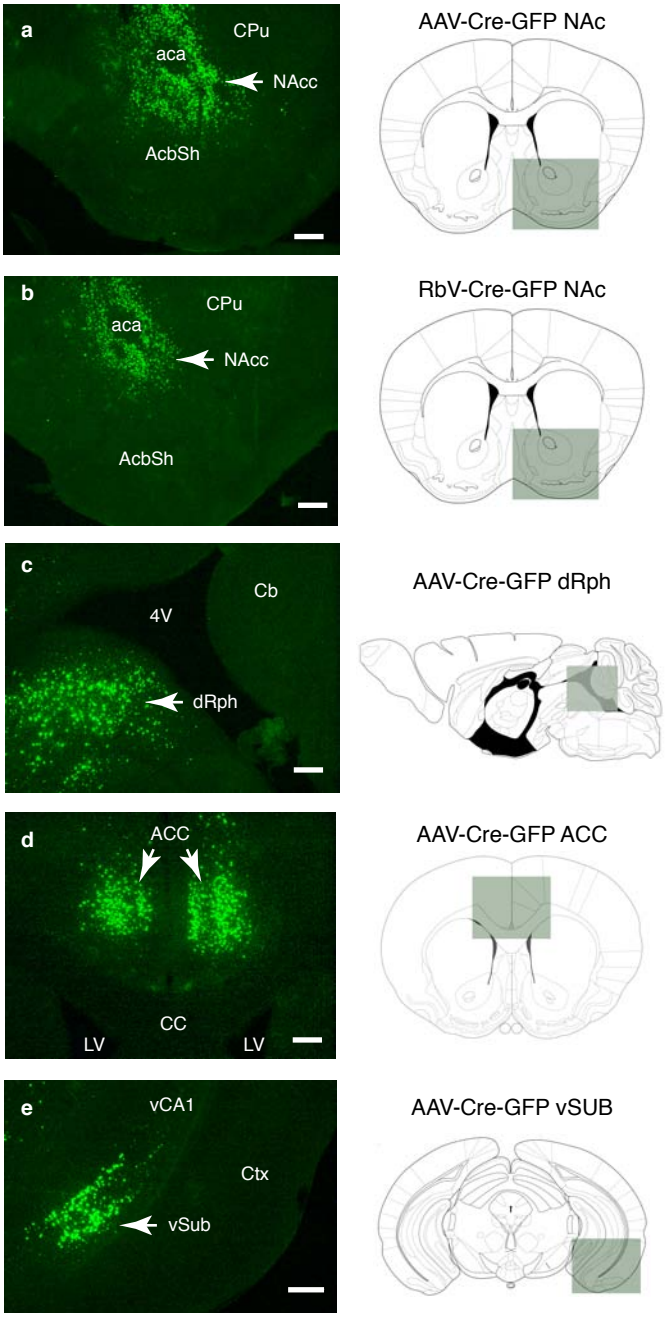

Supplementary Figure 10. Post-hoc confirmation of viral injection sites and transgene expression. a,b Localization and expression of (**a**) AAV-Cre-GFP and **(b)** RbV-Cre-GFP stereotaxic injections into the NAc. **c,d,e**, Localization and expression of AAV-Cre-GFP stereotaxic injections into the (**c**) dRph, (**d**) ACC and (**e**) vSub. (Nucleus accumbens core, NAcc; nucleus accumbens shell, AcbSh; anterior commissure, aca; caudate putamen a.k.a. dorsal striatum, CPu; dorsal Raphe, dRph; fourth ventricle, 4V; cerebellum, Cb; anterior cingulate cortex, ACC; corpus callosum, CC; lateral ventricle, LV; ventral subiculum, vSub; ventral CA1 region of the hippocampus, vCA1; entorhinal cortex, Ctx; Scale bars 250 μm)

Supplementary Figure 11

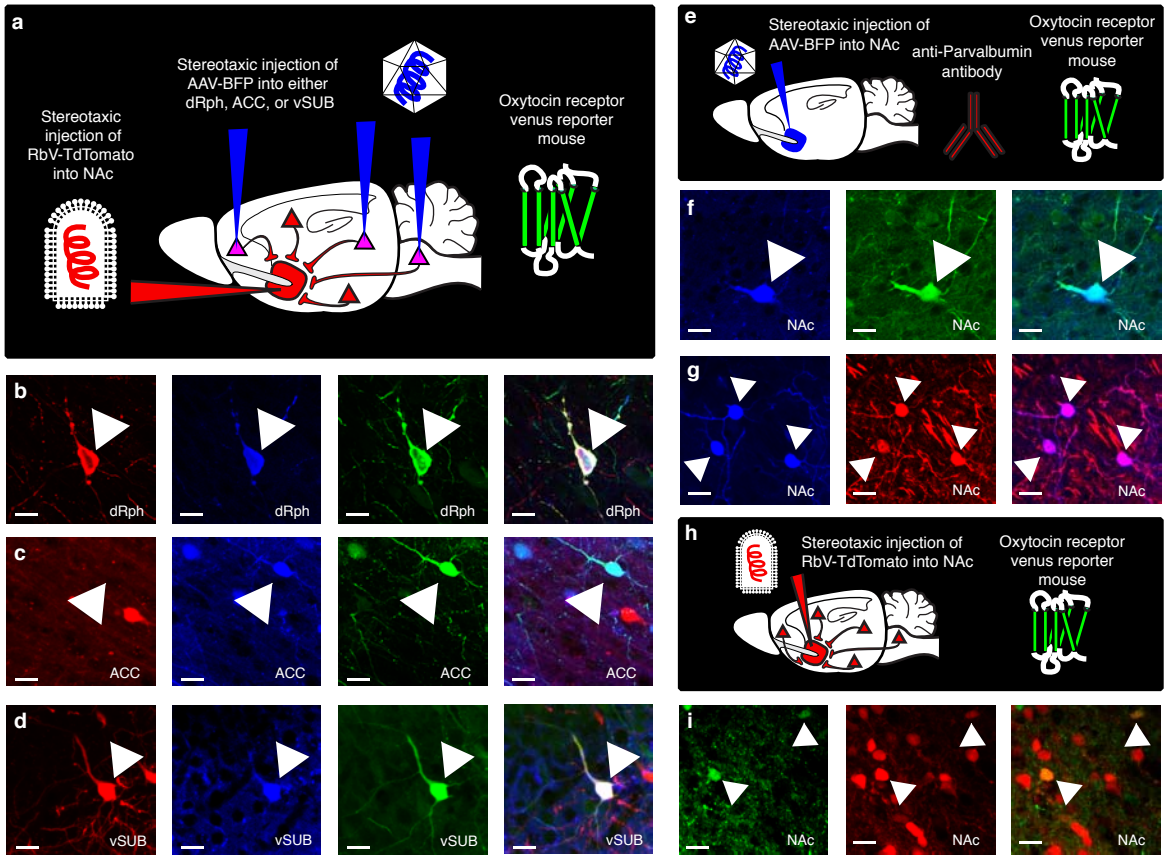

Supplementary Figure 11. Confirmation of viral tropism for OTR-expressing and NAc-projecting cells. a, Diagram illustrating stereotaxic injection of RbV-TdTomato into the NAc of OTR-Venus mice followed by AAV-BFP expression in either dorsal Raphe nucleus, dRph, anterior cingulate cortex, ACC or ventral subiculum, vSub shown in (**b-d**). **b-d,** high magnification images of cells in the (b) dRpH (c) ACC or (d) vSUB that have been retrogradely labeled by RbV-GFP taken up by presynaptic terminals in the NAc (red, left panels), labeled by local infection with AAV-BFP (blue, center left), and that express OTR-Venus (green, center right panels). Clear co-localization (merge, right panels) between RbV-TdTomato, OTR-Venus and AAV-BFP is evident in (b and d) and co-localization between OTR-Venus and AAV-BFP is evident (c). **e,** Diagram illustrating stereotaxic injection of AAV-BFP into the NAc of OTR-Venus mice or WT mice followed by subsequent immunohistochemistry with anti-Parvalbumin antibody shown in (**f-g**). **f,** Local infection with AAV-BFP (blue, left) in cells that express OTR-Venus (green, center). Co-localization (merge, right) indicates AAV tropism for OTR expressing cells in the NAc. **g,** Local infection with AAV-BFP (blue, left) in cells that express Parvalbumin (red, center). Co-localization (merge, right) indicates AAV tropism for Parvalbumin expressing cells in the NAc. **h,** Diagram illustrating stereotaxic injection of RbV-TdTomato into the NAc of OTR-Venus mice shown in (i). **i,** Local infection with RbV-TdTomato (red, left) in cells that express OTR-Venus (green, center). Co-localization (merge, right) indicates RbV tropism for OTR expressing cells in the NAc. (Scale bars 20 μm).

Supplementary Figure 12

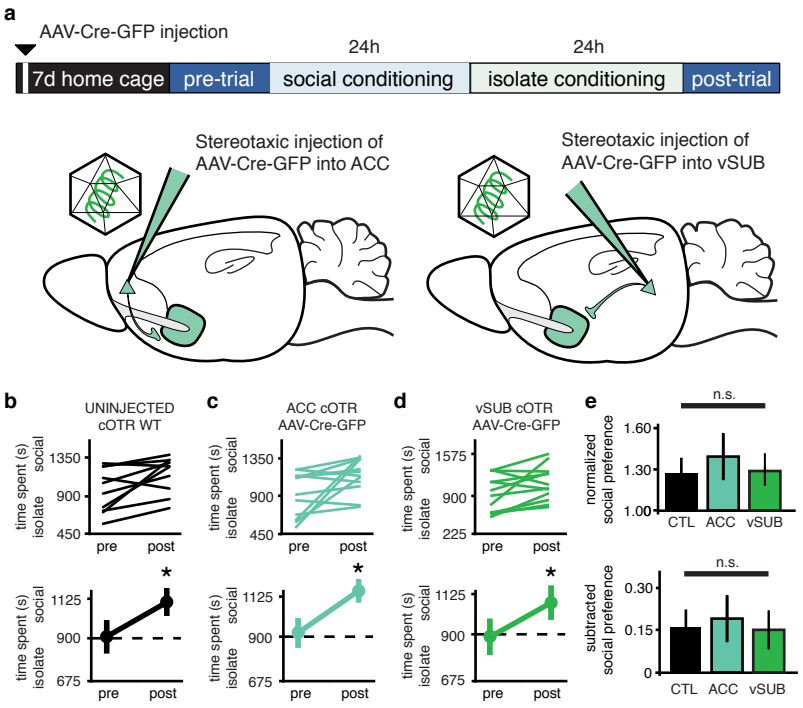

Supplementary Figure 12. ACC and vSub OT receptors (OTRs) are not required for sCPP. a, Diagram illustrating time course of viral injections into the ACC and vSub for sCPP experiments in **b-e**. **b,c,d** Individual (top) and average (bottom) preference scores indicate that un-injected cOTR KO animals (**b**), cOTR KO animals injected with AAV-Cre-GFP into the ACC (**c**) and cOTR KO animals injected with AAV-Cre-GFP into the vSub (**d**) have increased preference for the social bedding cue after conditioning (un-injected cOTR KO, n = 10, cOTR KO AAV-Cre-GFP ACC, n = 12, cOTR KO AAV-Cre-GFP vSub, n = 12). **e**, Comparisons between un-injected cOTR KO versus cOTR KO animals injected with AAV-Cre-GFP into the ACC or vSub reveals no difference in normalized social preference and subtracted social preference.

Supplementary Figure 13

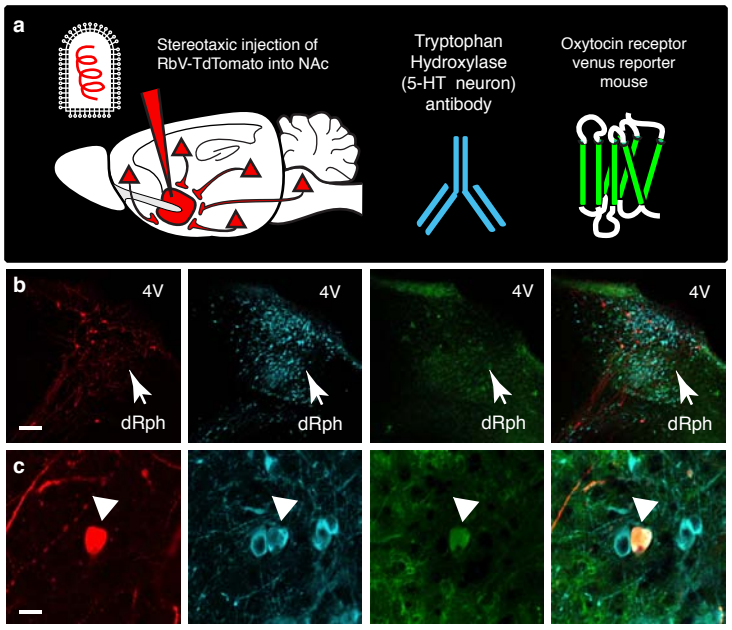

Supplementary Figure 13. OT receptor-expressing cells in the dRph send serotonergic projections to the NAc. a, Diagram illustrating stereotaxic injection of RbV-TdTomato into the NAc of OTR-Venus reporter mice, followed by subsequent immunohistochemistry with anti-tryptophan hydroxylase antibodies to label serotonergic neurons of the dRph. **b,c,** Low magnification (**b**, scale bar 200 µm) and high magnification (**c**, scale bar 20 µm) images of neurons in the dRph that send projections to the NAc (red, left), express OTR (green, middle left) and produce 5-HT (blue, middle right). Arrowheads and merged image (right) shows subset of neurons that show colocalization. (dorsal raphe, dRph; fourth ventricle, 4V).

Supplementary Figure 14

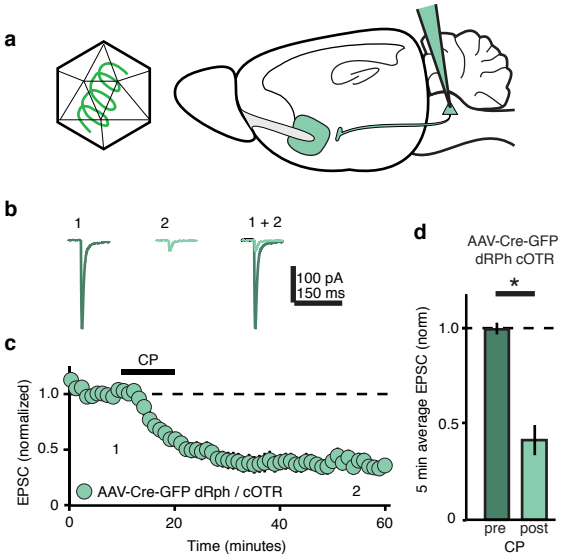

Supplementary Figure 14. OT does not alter inhibitory postsynaptic currents (IPSCs) recorded from NAc MSNs. a, Diagram illustrating time course of viral injections into the dRph for LTD experiments in **b-d**. Representative traces **(b)**, summary time course **(c)** and average post-treatment magnitude comparisons **(d)** reveal 5HT1b induced-LTD in EPSCs recorded from cOTR animals whose OTRs had been molecularly ablated by AAV-Cre-eGFP dRph injection (dRph-AAV-Cre-eGFP injected cOTR, n = 5 cells).

Supplementary Figure 15

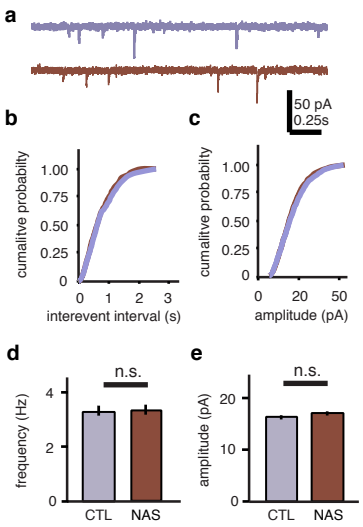

Supplementary Figure 15. 5HTR1b-A alone does not alter mini EPSC frequency or amplitude. **a**, Representative miniature EPSCs (mEPSCs) recorded in control neurons (purple) and neurons treated with NAS-181 (red, 20 µM, 10 minutes). **b**, Cumulative probability (top) and average (bottom) mEPSC frequency is decreased in OT-treated cells compared to control cells (control, n = 10, NAS-181, n = 10 cells). **c**, Cumulative probability (top) and average (bottom) mEPSC amplitude is not different in OT treated cells compared to control cells.

Supplementary Figure 16

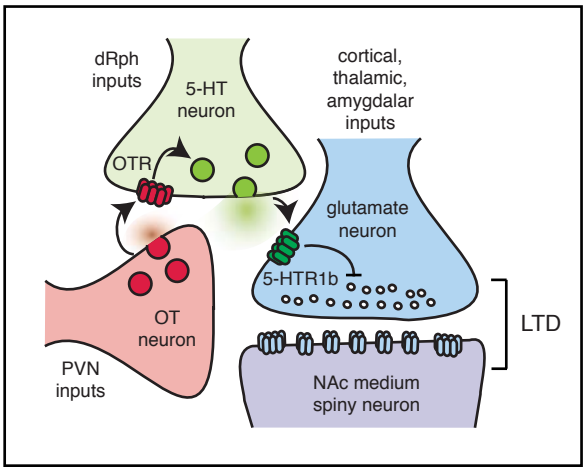

Supplementary Figure 16. Diagram illustrating model for induction of OT-induced LTD in NAc. OT producing neurons from the PVN release OT into the NAc. Activation of OTRs on presynaptic terminals of 5-HT neurons from the dRph causes the release of 5-HT into the NAc. Activation of 5HT1b receptors on glutamatergic terminals from various brain regions (cortex, amygdala, thalamus) decrease presynaptic function at excitatory synapses onto MSNs.